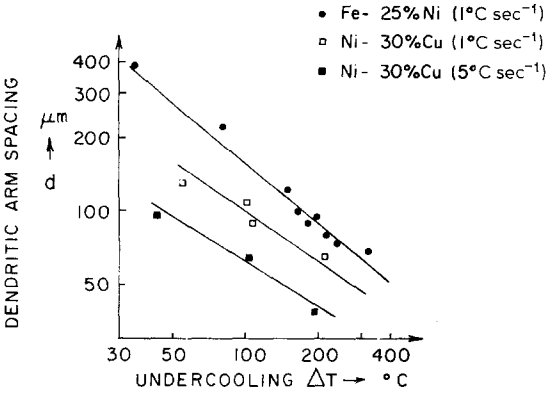

Figure 1 Dendritic arm spacing versus undercooling at different cooling rates for Ni–30% Cu [3] and Fe–25% Ni [4].

that the dendrite arm spacing is proportional to the solidification time t^p, where p is an empirical exponent. If we assume that the solidification time is almost equivalent to the time during coarsening, t_c, the dendrite arm spacing should be proportional to $[1/2(T_l - T_s)t_c]^p$ where T_l and T_s are the liquidus and solidus temperatures. Assuming that the time for recalescence is much smaller than the time for coarsening, the term $1/2(T_l - T_s)t_c$ represents approximately the area of the cooling curve during the coarsening time and between the two isotherms. It was also observed that coarsening at high temperatures requires less time than at lower ones, therefore final dendrite arm spacing should be proportional to $(\int T_m \mathrm{d}t_c)^p$ where T_m is the temperature of the melt.

Generally if both undercooling ΔT_u and coarsening cooling rate $\dot{T}_c$ are to be included in a single formula we can use the equation

$$d = C(\Delta T_u)^{-m}(\dot{T}_c)^{-n} \quad (6)$$

in which C is also an empirical constant. If we accept that the cooling rate is high and the undercooling is low, we will have $\Delta T_u \sim \dot{T}_u^{1/2}$; therefore Equation 6 becomes

$$d = c(\dot{T}_u)^{-m/2}(\dot{T}_c)^{-n}. \quad (7)$$

Applying this equation to the systems Fe–25% Ni [4] and Ni–30% Cu [3], we can find from Figure 1 that m is between $\frac{1}{2}$ and $\frac{1}{3}$. The same value of m was found for Ni–20% Cu [3].

In conclusion it is found that for powdered Fe–25% Ni conduction cooling is negligible, the dominant cooling being due to convection. For large ingots, however, the dendrite arm spacing is inversely proportional to the undercooling with a proportionality constant between $\frac{1}{2}$ and $\frac{1}{3}$.

References

1. COSTAS ACRIVOS, *J. Mater. Sci.* **11** (1976) 1159.
2. S. K. BHATTACHACYYA, J. H. PEVEPEZKO and T. B. MASSALSKI, *Acta Met.* **22** (1974) 879.
3. WALTER MOHN, Master Thesis University of Connecticut (1974).
4. T. Z. KATTAMIS, Ph.D. Thesis, Massachusetts Cambridge, Mass. (1965).

Received 28 May
and accepted 7 July 1976

COSTAS ACRIVOS
PAUL WILSON
Department of Metallurgy and Institute of Materials Science, University of Connecticut, Storrs, Conn, USA

A note on the residual stress about a pointed indentation impression in a brittle solid

The residual stress about a permanent hardness impression in brittle solids is of considerable importance to practical and theoretical aspects of indentation fracture mechanics. Lawn and Swain [1], and Lawn *et al.* [2] have previously described the role of the stress field about a pointed indenter in the initiation and propagation of so-called "median" or normal cracks on loading, and "radial" and "lateral" cracks on unloading. In particular, the residual stress provides the driving force for lateral cracking which is primarily responsible for the observed high two- and three-body abrasive wear rates of brittle solids. Thus any complete theoretical fracture mechanics description of these types of cracks must incorporate the residual stress. The residual stress is also important because of the increasing use of pointed indenters to notch brittle solids prior to bend strength determinations [3–5]. The residual stress about the permanent impression would be expected to

contribute to the magnitude of the crack tip stress intensity factor.

Indentation of brittle materials with a Knoop or Vickers pyramid has been found by many authors [3–8] to provide a convenient means of introducing a starting flaw for obtaining reproducible fracture mechanics parameters of brittle solids in flexure. However, systematic studies by some of these authors [3, 4, 7] were able to show that the critical stress intensity factor in flexure, K_{BC} determined using this approach was consistently lower than using alternative methods (e.g. double torsion, double cantilever). Moreover, it was found that when either the hardness impression was ground away [3] or annealed [3, 4, 7] that the new K_{BC} value determined in bending with the notched bar and by alternative methods were in excellent agreement. The observation of the lower K_{BC} prior to annealing indicates that there is some residual tensile force acting across the crack mouth.

The above observations provide a means of determining the residual stress about the deformed zone surrounding an indentation impression. From the principle of stress superposition, the stress intensity factor at the crack tip is just the summation of the stress intensity due to bending plus that due to the residual stress, that is

$$K_I = K_{BC} + K_R = K_{1C} \text{ (equilibrium)}. \quad (1)$$

Following Petrovic *et al.* [3], the stress intensity factor in a notched beam in bending is

$$K_{BC} = \sigma M(\pi c/Q)^{1/2} \quad (2)$$

where σ is the outer fibre tensile stress, M is a numerical factor $\simeq 1.0$ for small flaws, c is the flaw depth and Q is a factor relating to flaw geometry, and for the materials given here is given by $(\pi/2)^2$ for near half-penny like ($\frac{1}{2}$p) surface cracks.

The component of the stress intensity factor due to the residual stress is not quite as straightforward but to a good approximation may be thought of as equivalent to a force P acting at the mid-point of the surface trace of the flaw created during indentation. Lawn and Fuller [9] have recently indicated that the stress intensity factor at the tip of a penny-shaped (1p) crack during pointed indentation fracture is,

$$K_I = \frac{2P_\perp}{(\pi c)^{3/2}} \quad (3)$$

where $P_\perp$ is the point force perpendicular to the crack mouth at the midpoint of the surface trace of the crack. For a smooth conical indenter of half angle ψ, $P_\perp$ is given by

$$P_\perp = \frac{P}{2 \tan \psi} \quad (4)$$

The stress intensity factor due to the residual stress would then be

$$K_R = \frac{2P_{R\perp}}{(\pi c)^{3/2}} \quad (5)$$

where $P_{R\perp}$ is the residual force normal to the crack.

A measure of the residual stress intensity factor may be obtained by knowing K_{BC} before and after annealing the indented material. Then from Equation 1, one obtains

$$K_R = (K_{BC})_f - (K_{BC})_i. \quad (6)$$

on the assumption that $K_R = 0$ after annealing; the subscripts f and i indicate final and initial values of the stress intensity factor respectively. Values of K_R are listed in Table I for a wide range of materials. The ratio of the residual stress intensity factor K_R to the critical stress intensity factor after annealing $(K_{BC})_f$, which at equilibrium equals K_{1C}, is from Equations 3 and 5* given by

$$\frac{K_R}{K_{1C}} = \frac{2P_{R\perp}}{(\pi c)^{3/2}} \cdot \frac{(\pi c)^{3/2}}{2P_\perp} = \frac{P_{R\perp}}{P_\perp}. \quad (7)$$

Values of the ratio K_R/K_{1C} are listed in Table I and for the materials considered the ratio appears to be a constant independent of the hardness of the material. The possible exception is the lithium aluminium silicate glass ceramic which was annealed under load [5]. This may have caused some blunting of the crack tip, explaining the slightly higher K_R/K_{1C} value. The residual force $P_{R\perp}$ may be obtained from Eqution 7 upon substituting for $P_\perp$ from Equation 4, that is

*Strictly speaking, Equations 3 and 4 only apply for conical indenters, yet the data of Petrovic *et al.* [3] and Ingelstrom and Nordberg [7] for the depth of flaws as a function of load with a Knoop indenter, fits Equations 4 and 5 surprisingly well.

TABLE I Values of the hardness, critical stress intensity factor and residual stress intensity factor for a number of materials

Material	Hardness (GPa)	$(K_{BC})_f$ (after anneal) ($MN\,m^{-3/2}$)	$(K_{BC})_i$ (before anneal) ($MN\,m^{-3/2}$)	K_R ($MN\,m^{-3/2}$)	K_R/K_{1C} $MN\,m^{-3/2}$)	Reference
Lithium aluminium silicate	$\sim$ 12–13	0.76	0.47	0.29	0.38	5
SiC	$\sim$ 30	3.8	2.57	1.23	0.32	4
Si_3N_4	$\sim$ 22	4.65	3.4	1.25	0.27	3
WC(Co)	17.0	10.0	6.9	3.1	0.31	7
WC(Co)	–	11.0	8.5	2.5	0.23	7
WC(Co)	15.5	12.3	8.6	3.7	0.30	7
				Mean K_R/K_{1C} = 0.30		

$$P_{R\perp} = \frac{K_R}{K_{1C}} \cdot \frac{P}{2 \tan \psi} . \quad (8)$$

The residual force may be converted into an equivalent stress if we know the area over which it operates. Previously [1] it has been shown that it is convenient to represent the mean indentation pressure or hardness by

$$p_0 = P/\alpha \pi a^2 = H, \quad (9)$$

where α is a dimensionless constant determined by the indenter geometry (for a Vickers pyramid $\alpha = 2/\pi$ with a the half diagonal of indentation). A similar expression for the residual stress σ_R may be written if it is assumed that in the case of a Vickers pyramid impression the residual force acts through a semicircle of radius a (the half diagonal of indentation) then

$$\sigma_R = P_{R\perp}/\pi a^2 . \quad (10)$$

This assumption is reasonable for materials with a high ratio of yield stress (or hardness) to Young's modulus ($Y/E > 1/20$). Now combining Equations 8, 9 and 10 we have

$$\sigma_R = \frac{K_R}{K_{1C}} \frac{H}{\tan \psi} \quad (11)$$

A similar expression may be obtained for a Knoop indenter if a in Equation 10 is taken as half the mean of the two diagonals. For a Knoop indenter $\tan \psi \simeq 2$ and the mean value of $K_R/K_{1C} \simeq 0.3$ giving a value of $\sigma_R \simeq H/20$.

It is not clear at this stage just why the ratio of K_R/K_{1C} appears to be a constant independent of material. More recent work [10] indicates that the ratio of K_R/K_{1C} is almost independent of load until high indenter loads are reached at which point the residual stress intensity factor approaches zero. This may be due to extensive crushing under the indenter or relief of the residual stress by lateral cracking.

Acknowledgements

The author acknowledges informative discussions with J.T. Hagan and comments on the manuscript by B.R. Lawn. The S.R.C. is thanked for financial support.

References

1. B. R. LAWN and M. V. SWAIN, *J. Mater. Sci.* **10** (1975) 113.
2. B. R. LAWN, M. V. SWAIN and K. PHILLIPS, *ibid.* **10** (1975) 1236.
3. J. J. PETROVIC, L. A. JACOBSON, P. K. TALTY and A. K. VASUDERAN, *J. Amer. Ceram. Soc.* **58** (1975) 113.
4. J. J. PETROVIC and L. A. JACOBSON, *ibid* **59** (1976) 34.
5. K. R. KINSMAN, R. K. GOVILA and P. BEARDMORE, "Deformation of Ceramic Materials", edited by R. C. Bradt and R. E. Tressler (Plenum Press, New York, 1975) p. 465.
6. R. K. GOVILA, *Acta Met.* **20** (1972) 447.
7. N. INGELSTROM and H. NORDBERG, *Eng. Fract.*

Mechs. **6** (1974) 597.
8. P. KENNY, *Powder Met.* **14** (1971) 22.
9. B. R. LAWN and E. R. FULLER, *J. Mater. Sci.* **10** (1975) 2016.
10. M. G. MENDIRATTA and J. J. PETROVIC, *ibid* **11** (1976) 973.

Received 9 June
and accepted 8 July 1976

M. V. SWAIN
Physics and Chemistry of Solids Section, Cavendish Laboratory, University of Cambridge, UK

Transition from slow to fast crack propagation in PMMA

It is a well-known feature of the fracture behaviour of PMMA that at the critical value of stress intensity factor, K_{IC}, a jump in the crack speed is observed (Fig. 1). Typically for PMMA at room temperature the crack speed jumps from about 0.1 to about 10 to 100 m sec^{-1} depending on testing conditions. Associated with this jump is a significant change in the fracture surface morphology, which can be seen in Fig. 2. The crack propagation direction is from left to right: the slow crack propagation region appears rough and there is an abrupt transition to the smooth high speed region.

Two mechanisms have been suggested to account for this crack speed behaviour. The first,

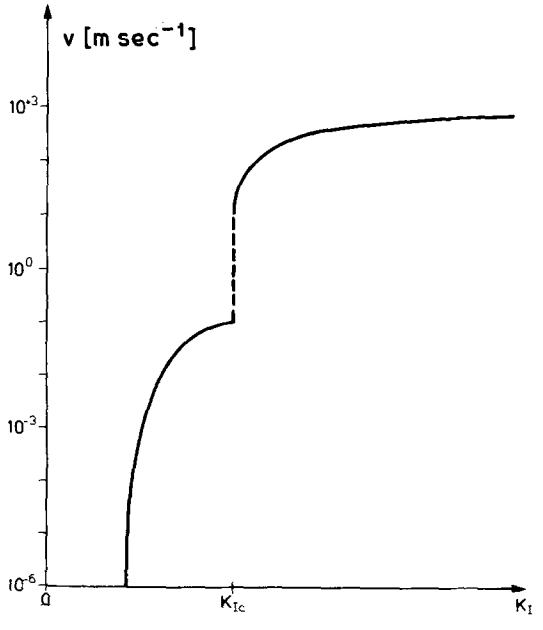

Figure 1 Crack speed v versus stress intensity factor K_I in PMMA (schematic representation).

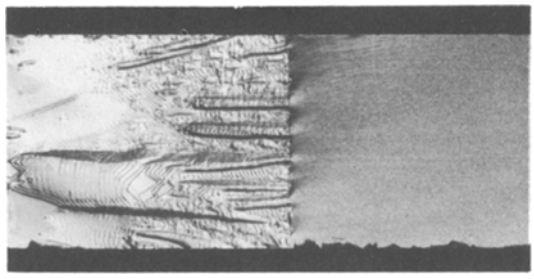

Figure 2 Fracture surface of PMMA $M_w = 8\,000\,000$ showing transition from slow to fast crack propagation. Specimen thickness shown corresponds to 4.16 mm (crack propagation direction from left to right)

by Williams [1, 2] explains the jump in crack speed as being due to a change-over from isothermal to adiabatic conditions at the tip of a crack in a certain range of crack speeds. Thus, the heat generated by the plastic deformation process at the crack tip builds up in the crack tip region, leading to a rise in temperature and a consequent softening of the material and a reduction in its resistance to fracture.

In the second mechanism, Johnson and Radon [3, 4] invoked the β-relaxation in PMMA, which is attributed to the relaxation of the ester side groups, to explain the transition in crack speed behaviour. Although no detailed mechanism was put forward coupling the relaxation to crack tip processes the theory was substantiated by the correlation between the temperature dependence of a "time to failure" inferred from fracture experiments and the temperature variation of the reciprocal frequency of the β-relaxation peak.

Support for both these mechanisms is to be found in the literature. One of the present authors [5], for instance, used the model of a moving cylindrical heat source of Weichert and Schönert [6] in the context of an isothermal–adiabatic transition to calculate bounds to the crack speed immediately prior to the transition and found a